Structure of outer membrane protein A transmembrane domain by NMR spectroscopy

Ashish Arora[1], Frits Abildgaard[2], John H. Bushweller[1] and Lukas K. Tamm[1]

[1]*Department of Molecular Physiology and Biological Physics, University of Virginia, Charlottesville, Virginia 22908-0736, USA.* [2]*NMRFAM, University of Wisconsin, Madison, Wisconsin 53706, USA.*

We have determined the three-dimensional fold of the 19 kDa (177 residues) transmembrane domain of the outer membrane protein A of *Escherichia coli* in dodecylphosphocholine (DPC) micelles in solution using heteronuclear NMR. The structure consists of an eight-stranded β-barrel connected by tight turns on the periplasmic side and larger mobile loops on the extracellular side. The solution structure of the barrel in DPC micelles is similar to that in *n*-octyltetraoxyethylene (C_8E_4) micelles determined by X-ray diffraction. Moreover, data from NMR dynamic experiments reveal a gradient of conformational flexibility in the structure that may contribute to the membrane channel function of this protein.

Multidimensional heteronuclear NMR spectroscopy has become a major technique for determining the structure and dynamics of macromolecules in solution[1,2]. These techniques were limited to soluble proteins and nucleic acids because of the well-known size limitation of high resolution NMR. The structures of two transmembrane (TM) peptides have been solved recently by solution NMR. In a breakthrough study, the structure of the TM domain of glycophorin (a dimer of 40 residues) has been determined in dodecylphosphocholine (DPC) micelles[3]. The structure of the TM subunit c of the F_1F_0-ATP synthase (79 residues), which forms a helical hairpin has been solved in a mixture of organic solvent and water at two different pHs[4]. However, no larger membrane protein structures have so far been determined by NMR. Although solid state NMR has no theoretical size limit, it has other experimental difficulties to overcome. Currently, the structures of the gramicidin channel[5] and a channel-lining segment from the acetylcholine receptor[6] have been determined using solid state NMR. Searches of genome-wide databases revealed that ~30–40% of all proteins in eukaryotic cells are expected to be membrane proteins. Because it is difficult to grow crystals of membrane proteins that are suitable for X-ray diffraction, solution NMR may become a viable alternative for solving membrane protein structures if the current size limit can be increased.

Several recent developments create considerable hope for the feasibility of solving the structures of integral membrane proteins by NMR. TROSY-based methods[7] provide a substantial improvement in the relaxation behavior of the ^{15}N nuclei, especially at the high field strengths that are now available (900 MHz). The folds of large proteins and complexes can be obtained from samples with deuterated side chains[8]. Partial protonation of the side chains yields additional distance constraints[9] and measurements of residual dipolar couplings provide orientational restraints[10], both of which result in higher resolution structures of such proteins. Long range distance constraints can be obtained with strategically placed spin labels[11] to further extend the size limit of solution NMR. Significant progress has also been made in the areas of high yield expression, purification and refolding of membrane proteins[12–14]. High yield expression and purification are essential for introducing ^{13}C, ^{15}N and ^{2}H in various patterns for NMR measurements.

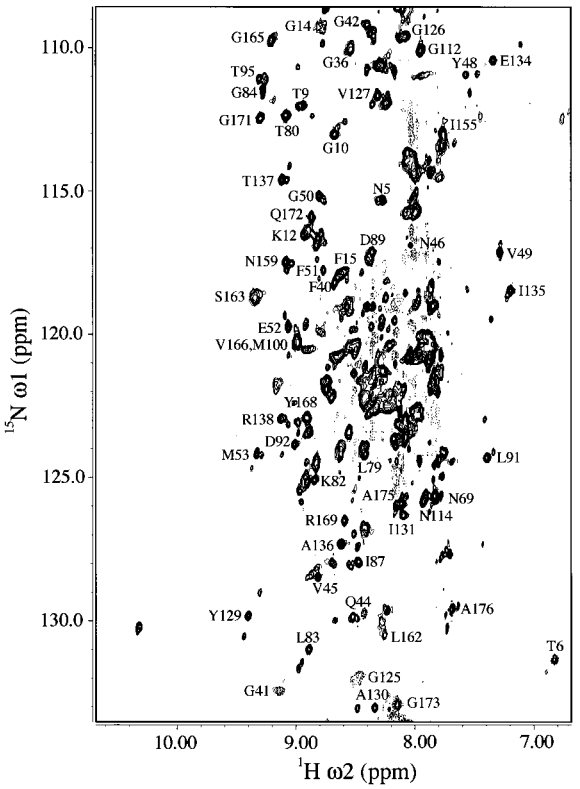

Fig. 1 TROSY-based ^{1}H-^{15}N HSQC spectrum of 1 mM OmpA(0–176) in 600 mM deuterated DPC micelles in 10 mM potassium phosphate buffer, pH 6.3 (containing 50 mM NaCl, and 0.1 % NaN_3). The spectrum was recorded at 50 °C on a 750 MHz spectrometer. Several of the assigned resonances are labeled.

The outer membrane protein A (OmpA) of *E. coli* has been used in our laboratory for several years as a model to study mechanisms of membrane protein folding[15,16]. Although OmpA most likely serves a physiological structural function in maintaining the proper shape of Gram-negative bacteria, it also forms ion channels in planar lipid bilayer membranes[17,18]. The channel activity provides a convenient functional assay to monitor the refolding of OmpA into its native state. OmpA is also one of the major surface antigens of Gram-negative bacteria and, thus, is an important target in the immune defense against many bacterial pathogens[19,20]. The 35 kDa OmpA protein consists of a TM domain (19 kDa) and a globular periplasmic domain (16 kDa). The crystal structure of the TM domain of OmpA in C_8E_4 detergent micelles has recently been solved by X-ray crystallography[21,22]; it is a β-barrel. Since the crystal structure did not explain the channel function of OmpA, we decided to solve the structure in DPC micelles by solution NMR. The general fold of the β-barrel is similar in both the crystal and solution structures; however, NMR also detected dynamic gradients along the barrel axis that may contribute to the structural features of OmpA function as a surface antigen and membrane channel.

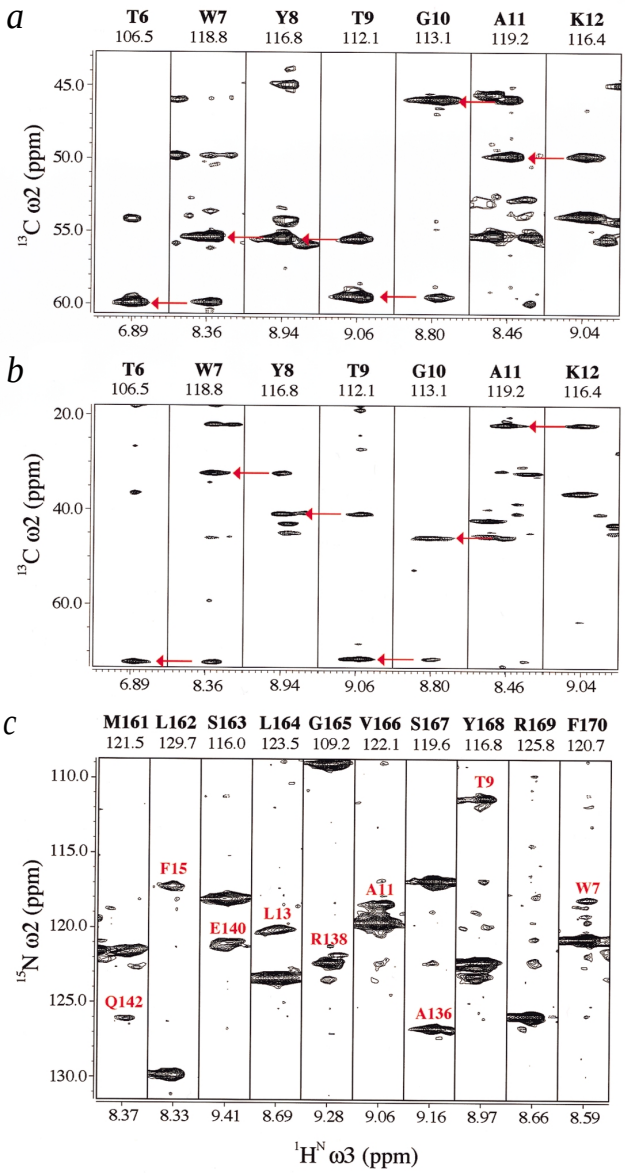

Fig. 2 Sequential assignment of OmpA(0–176). Selected strips from ***a***, a TROSY-based 3D HNCA. ***b***, a TROSY-based 3D HN(CA)CB spectrum of refolded OmpA (0–176) (1 mM) in 600 mM DPC micelles showing the sequential assignments (arrows) of residues 6–12 in the first β-strand. ***c***, Strips from a ^{15}N-edited HSQC-NOESY-HSQC spectrum of OmpA(0–176) in DPC micelles showing HN–HN NOE connectivities between strands β8 and β1 or β7. The spectra in (*a*) and (*b*) were recorded at 750 MHz and the spectrum in (*c*) was recorded at 600 MHz.

Expression, refolding, and conditions for NMR spectroscopy

The TM domain of OmpA [OmpA(0–176)] was expressed in BL21(DE3) cells under the control of the T7 promoter. Deletion of the signal sequence and expression into inclusion bodies increased protein yields ~10-fold and was necessary to obtain sufficient amounts of isotope-labeled protein at a reasonable cost. Both the protein purified from inclusion bodies and that isolated from outer membranes[17] displayed the same refolding behavior in DPC micelles (data not shown). TROSY-based ^{15}N-^{1}H HSQC spectra of ^{15}N-labeled OmpA(0–176) were used to optimize conditions of sample composition and temperature. The best results were obtained at 1 mM OmpA(0–176), 600 mM DPC and 50 °C. Consistent with earlier observations of high heat resistance[23,24], the protein showed no signs of degradation at this temperature even after many weeks of measuring time.

Sequential resonance assignments

Sequential resonance assignments were obtained from TROSY-based HNCA, HN(CA)CB, HNCO, and HN(CA)CO[25,26] experiments at 600 and 750 MHz. Specifically ^{15}N-labeled Ala, Arg, Asn, Gln, Ile, Leu, Lys, Phe, Thr, Trp, Tyr and Val samples helped with the assignment process. These spectra showed signs of exchange broadening for several residues, most notably in the vicinity of the Trp residues. Exchange broadening in the vicinity of Trp has been documented before for other proteins[27]. This problem was alleviated in a single Trp mutant OmpA(0–176) in which four of the five Trp residues were replaced by Phe. A TROSY-based ^{15}N-^{1}H HSQC spectrum of refolded Trp 7 OmpA(0–176) is shown in Fig. 1. Strips of HNCA and HN(CA)CB spectra demonstrating the sequential assignments of residues 6–12 are shown in Fig. 2*a*,*b*.

Complete backbone resonance assignments (HN, N, CA, CB and CO) were obtained for a total of 138 of the 177 residues (18 more residues were partially assigned) resulting in the identification of eight β-strands based on ^{13}C chemical shifts and NOEs. Some Hα assignments were obtained from NOESY spectra of a 50% deuterated sample. Characteristic HN–HN inter-strand NOEs in the ^{15}N-edited NOESY-TROSY[28] and HSQC-NOESY-HSQC[29] data identified the antiparallel orientation of the strands and established the closed barrel topology of the protein (see below). The tight turns of 3–4 residues connecting the strands on the periplasmic end of the barrel were well-defined. However, significant difficulty was encountered in assigning the resonances of the longer loops at the extracellular end. Proceeding from the middle of each of the strands to either end, the line width increased and the performance of the triple-resonance spectra decreased due to dynamic broadening (see below). The extracellular loops were particularly affected, resulting in very weak or missing peaks for a number of residues in these regions.

Additional challenges were presented by the presence of a second set of peaks with ~20% of the intensity of the major species. The chemical shifts were virtually identical for these peaks, but they were displaced slightly in the ^{15}N and HN dimensions. Virtually all peaks displayed a second peak of weaker intensity. The percentage of this second species was insensitive to detergent-to-protein ratio, protein concentration or temperature. The samples with specifically ^{15}N-labeled residues greatly facilitated unambiguous assignments of these complex spectra. Although the source of this doubling has not yet been identified, it is possible that the second set of peaks represents a minor conformation of the protein.

Collection of data for structure calculations

The ϕ and ψ angles predicted from the chemical shifts of Cα, Cβ and CO confirmed the presence of eight β-strands that were interrupted by alternating long and short irregular sequences. The predicted β-strands were further scrutinized for short and long range NOEs measured from ^{15}N-edited NOESY-TROSY and ^{15}N-edited HSQC-NOESY-HSQC spectra. In addition to HN–HN NOEs between neighboring β-strands, several strong HN–HN NOEs were found between strands β1 and β8, indicating the existence of a closed eight-stranded β-barrel (Fig. 2*c*). Standard hydrogen bond restraints were added to those residues

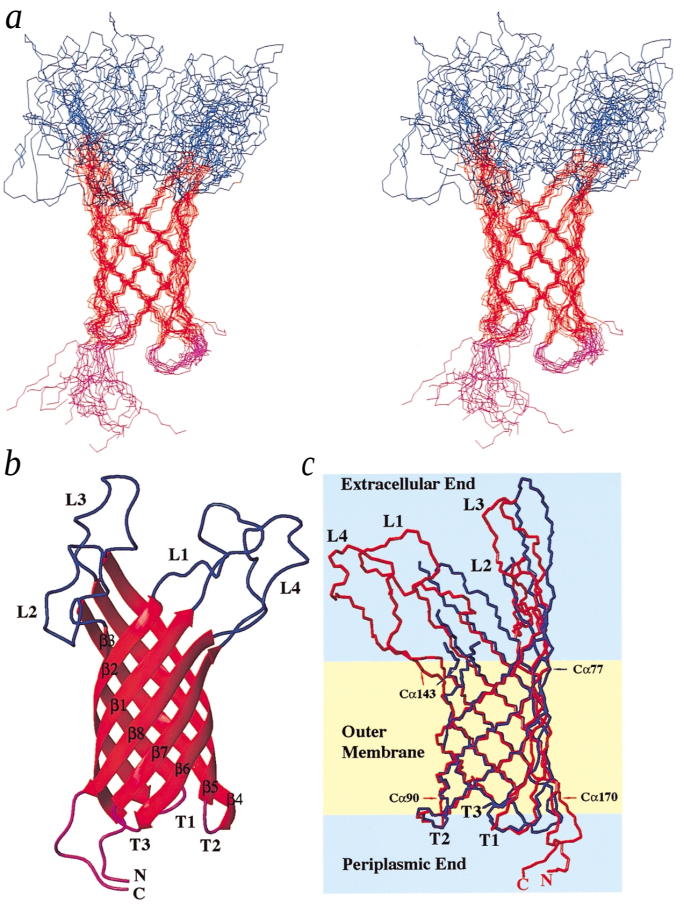

Fig. 3 Solution structure of OmpA TM domain in detergent micelles. ***a***, Stereoview of the 10 lowest energy conformers representing the NMR solution structure of OmpA(0–176) in D38-DPC micelles. The β-strand regions are shown in red, the loop regions in blue and the turns and N- and C-termini in purple. ***b***, Ribbon representation of OmpA(0–176) in DPC micelles produced with the program MOLMOL[40]. The color scheme is as described in (*a*). The eight β-strands (β1–β8), four extracellular loops (L1–L4), and three periplasmic turns (T1–T3) are labeled. ***c***, Comparison of the NMR detergent micelle (red) and X-ray crystal (blue) structures of the OmpA TM domain. The positions of the α-carbons of four residues are labeled for reference.

that were identified by the above procedure to be part of the β-barrel.

Based on 49 HN–HN and 42 HN–Hα experimental NOE-derived distance constraints, 71 ϕ and 71 ψ dihedral angle constraints and constraints for 58 hydrogen bonds, the fold of OmpA(0–176) was calculated and energy minimized (Table 1). Backbone traces of the 10 lowest energy structures are shown in Fig. 3*a*; a minimum of 82 residues are in β-strands in all average structures. The backbone root mean square (r.m.s.) deviation over these 82 residues is 1.19 ± 0.29 Å, and the r.m.s. deviation over all heavy atoms is 2.24 ± 0.45 Å. The definition of the short turns is good, but that of the long loop regions is significantly poorer due to the lack of assignments and constraints for these regions.

NMR solution structure in detergent micelles

The lowest energy NMR solution structure of OmpA(0–176) in DPC micelles is a well-defined eight-stranded antiparallel β-barrel (Fig. 3*b*). The residues forming the eight strands (numbered β1–β8) are: β1, 6–16; β2, 34–45; β3, 49–57; β4, 75–86; β5, 91–103; β6, 117–130; β7, 135–142; and β8, 161–169. The six N-terminal and the six C-terminal residues are unstructured and are at the periplasmic side of the barrel. Three well-defined turns at the periplasmic end (bottom of Fig. 3) and four long unstructured loops at the extracellular end (top of Fig. 3) connect the strands. The loops extend from residues 17–33 (L1), 58–74 (L2), 104–116 (L3) and 143–160 (L4). Most of the amide protons of assigned loop residues showed no HN–Hα NOEs, but had crosspeaks with water, consistent with a water-exposed mobile protein domain.

The eight-stranded β-barrel conformation found by NMR closely resembles the structure obtained by X-ray diffraction[22]. For comparison, the crystal structure and the lowest energy micelle structure are aligned in Fig. 3*c*. The r.m.s. deviation between the NMR and X-ray structure coordinates is 1.28 Å for the 108 best-fitting barrel and turn residues (4–17, 34–57, 71–106, 118–141 and 161–170). The two structures have the same barrel dimensions, similar tilt angles for the β-strands, the same shear number[30] of 10 and an elliptical cross section of the barrel. However, some β-strands extend further into the loops in the crystal structure than in the NMR structure. Compared to the crystal structure, strands β7 and β8 are one residue shorter and strands β3, β4, β5 and β6 are three residues shorter in the NMR structure. Irregular backbone conformations were found for Leu 58, Gly 59 and Arg 60 (β3); Tyr 72, Lys 73 and Ala 74 (β4); Ala 104, Asp 105 and Thr 106 (β5); Asn 114, His 115 and Asp 116 (β6); Phe 143 (β7) and Phe 170 (β8).

Although the loops appear to be better defined in the crystal structure, the B-factors of the residues in the loop regions were quite high (Fig. 4*b*) and portions of the loops could not be identified in the electron density map[22]. It should also be noted that in order to grow crystals, three nonconservative mutations were engineered into loops L1, L2 and L3, respectively. The wild type protein apparently did not yield diffraction quality crystals. Whether these surface mutations locked the otherwise mobile loops into a more fixed conformation is not known.

Dynamics of OmpA TM domain in detergent micelles

To examine the conformational dynamics of the main chain, we measured heteronuclear NOEs in a 3D [^{1}H]-^{15}N NOE-HNCO-TROSY[31] experiment. Heteronuclear NOEs are very sensitive to the mobility of individual amide N-H bond vectors on a ps–ns time scale. The heteronuclear NOEs of 114 residues are plotted in Fig. 4*a*. The average values are 0.73 in the β-barrel, 0.67 in the turns and 0.46 in the loop regions. With a static limit of 1.0 for completely immobile residues, the values indicate a fairly rigid barrel with slightly flexible turns. The loop residues are clearly more mobile. For comparison, the local backbone r.m.s. deviations and global residue displacements calculated over the 10 minimum energy structures are plotted in Fig. 4*b* along with the B-factors obtained from X-ray diffraction[22]. The residues in the loops have high r.m.s. deviations resulting from a lack of distance constraints in this region. The high r.m.s. deviations correlate well with the low heteronuclear NOEs and high B-factors. Therefore, the loops of OmpA constitute a highly mobile domain that lacks a well-defined structure. The highly dynamic structure of these surface loops may explain the high immunogenicity of OmpA as a surface antigen.

A close examination of the shapes and intensities of the HSQC and HNCA resonances arising from residues in the β-barrel also suggests a dynamic profile on the μs–ms time scale. The intensi-

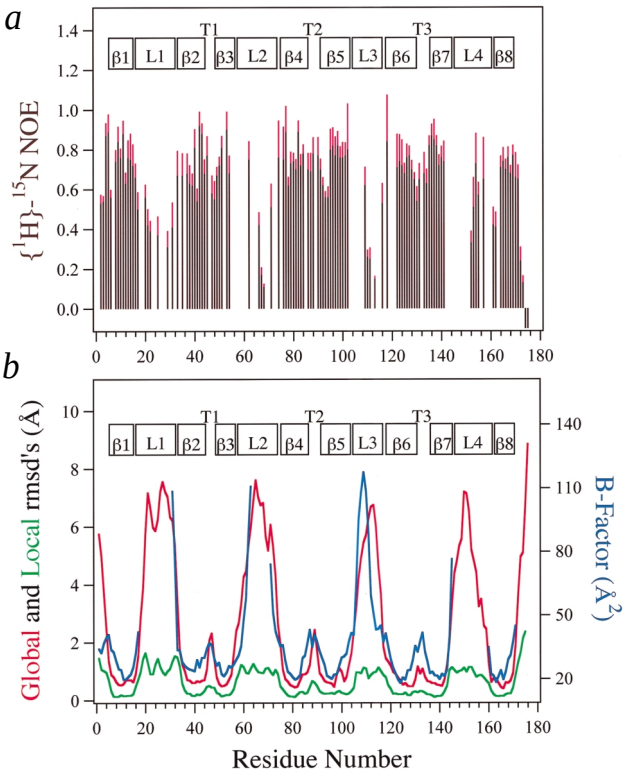

Fig. 4 Dynamics of OmpA TM domain in detergent micelles. ***a***,Heteronuclear {^{1}H}-^{15}N NOEs of OmpA TM domain plotted as a function of residue number. The positive standard deviations (calculated according to ref. 41) are shown in pink. ***b***, Global displacement (red) and local r.m.s. deviations (green) values for the backbone residues averaged over the 10 individual conformers representing the detergent micelle structure of OmpA(0–176). The B-factors (blue) of the Cα atoms of the 1.65 Å resolution crystal structure of OmpA(0–171) (ref. 22) are shown for comparison.

ties of the peaks decrease and the lines broaden towards both ends of the barrel. These effects are more pronounced toward the loops than toward the turns of the barrel. The same behavior is observed for the HN–HN NOE crosspeaks (see Fig. 2*c* for example). Therefore, a dynamic gradient exists along the axis of the barrel, with the most rigid backbone structure in the center. The center of the barrel exposes hydrophobic side chains to the outside and corresponds to the region that fits into the mid plane of the lipid bilayer. The more flexible barrel ends consist of aromatic and polar residues and are expected to be in contact with the polar head groups of the surrounding detergent or lipid molecules. A similar dynamic gradient has been observed by time-resolved fluorescence spectroscopy in a helical TM model peptide[32].

The ordered packing of the lipid bilayer may impose slightly different motional constraints on the protein dynamics than the environment of a detergent micelle. The motions in phospholipids in a lipid bilayer are more restricted than in detergents in a micelle. The differences are probably largest in the regions of the polar headgroups. Regardless of these secondary effects, the observed dynamic gradient in membrane proteins appears to counter a dynamic gradient in the lipids, which are most dynamic in the center of the bilayer[33]. Although the dynamic gradient that we have observed in OmpA could contribute to its ability to conduct ions across membranes, any mechanism would also have to take into account the extraordinary thermodynamic stability of the β-barrel portion of OmpA in membrane environments.

Conclusions

The success of our effort to determine the fold of the OmpA TM domain demonstrates that solution NMR methods can be used to obtain the 3D folds of membrane proteins on the order of 20 kDa in detergent micelles. In addition to structure determination, dynamic information on various time scales can be obtained by these methods. Thus, further applications of this approach to other membrane proteins would broaden our knowledge of the structures and functions of this class of proteins.

Methods

Mutagenesis, expression and labeling. The codon for Pro 177 in plasmids harboring wild type OmpA or the single tryptophan mutant, Trp 7 (ref. 15), was converted to a stop codon to yield the TM domain fragments of the protein[17]. The signal sequences of proOmpA were replaced by a methionine. The modified OmpA genes were subcloned into pET14b (Novagen) using the *Nco*I and *Nde*I sites, yielding pET112 and pET111, which express OmpA(0–176) and the Trp 7 mutant of OmpA(0–176), respectively, in BL21(DE3) cells under the control of the T7 promoter.

Uniformly ^{2}H-, ^{13}C-, and ^{15}N-labeled OmpA(0–176) was prepared by growing cells in 99.92% D_2O minimal media containing 2 g l^{-1} 98% ^{2}H-, ^{13}C-labeled D-glucose (MartekBio), 1 g l^{-1} ^{15}N-ammonium sulphate, and 1% CDN100-Bioexpress (Cambridge Isotopes). To produce 50% ^{2}H-, 98% ^{13}C-, ^{15}N-labeled proteins, 50% ^{2}H- and 98% ^{13}C-labeled D-glucose was used and the cells were grown in 50% D_2O-H_2O with 1% CDN50-Bioexpress. Specifically ^{15}N-labeled proteins were prepared in auxotrophic strains[34] in rich media including appropriate amounts of specific ^{15}N-labeled amino acids[35].

Purification. IPTG-induced cells were osmotically shocked and French-pressed to harvest inclusion bodies. The pellets were dissolved in 20 ml 20 mM Tris buffer, pH 8.0, containing 8 M urea. An equal volume of isopropanol was added, the suspension was brought to 55 °C for 30 min and centrifuged in a Beckman 45Ti rotor at 38,000 rpm for 90 min at 4 °C. The protein was purified using a 0–100 mM NaCl gradient in 15 mM Tris, pH 8.5, 0.1% β-mercaptoethanol, 8 M urea on a Q-Sepharose Fast Flow column. The purest fractions were pooled and concentrated to 30 g l^{-1} using Amicon PM-10 membranes.

Refolding and sample preparation for NMR experiments. Approximately 10 mg OmpA(0–176) in 0.3 ml 8 M urea was diluted into 20 ml 15 mM D38-DPC (Cambridge Isotopes) micelles in 20 mM sodium borate buffer, pH 10.0 (containing 150 mM NaCl, 1 mM EDTA). Refolding was monitored by CD spectroscopy and SDS-PAGE. The yields of refolding were 100%. The proteins were concentrated 40-fold with Amicon YM-1 membranes. The buffer was changed to 10 mM potassium phosphate, pH 6.3, 50 mM NaCl, 0.01 NaN_3 by two rounds of dilution and concentration. 25 µl D_2O was added to the final NMR samples.

NMR spectroscopy. NMR spectra were recorded on Varian Inova 500 and 600 MHz and Bruker DMX 750 MHz spectrometers equipped with 5 mm triple-resonance probes and z-only or triple-axis field gradients, respectively. ^{15}N-edited ^{1}H-^{1}H NOESY-TROSY[28] spectra of a 50 % ^{2}H-, 98 % ^{13}C-, ^{15}N-labeled sample were recorded at 750 MHz using a mixing time of 90 ms. ^{15}N-edited HSQC-NOESY-HSQC[29] spectra of a 98 % ^{2}H-, ^{13}C-, ^{15}N-labeled sample were recorded at 600 MHz using a mixing time of 200 ms. The 3D [^{1}H]-^{15}N NOE-HNCO-TROSY[31] experiment was recorded with a 5.4 s saturation delay (3× HN-T_1).

Structure calculations. Backbone dihedral angle restraints for φ

Table 1 Structural statistics for OmpA(0–176)

NOE distance constraints	91
HN–HN NOEs	49
HN–Hα NOEs	42
Hydrogen bond constraints	116
Angle Constraints	142
ϕ	71
ψ	71
NMR constraints violations	
NOE	
Sum (Å)[1]	0.93 ± 0.20 (0.6–1.24)
Maximum (Å)	0.09
Dihedral angle	
Sum (°)[1]	32.95 ± 4.6 (25.41– 38.63)
Maximum (°)[1]	1.8 ± 0.17 (1.56–2.13)
AMBER energy (kcal mol^{-1})[1]	–3100.96 ± 83.80 (–3293.00–3029.24)
R.m.s. deviation from the mean structure (Å)	
All residues	
Backbone atoms	4.73 ± 0.97
All heavy atoms	5.51 ± 1.05
Residues in β-strands[2]	
Backbone atoms	1.19 ± 0.25
All heavy atoms	2.24 ± 0.41
Ramachandran statistics[3]	
Residues in allowed region	95.7%
Residues in disallowed region	4.3%

[1]The values in parentheses are the observed ranges.
[2]Residues for calculating the r.m.s. deviations are 6–16, 34–44, 49–55, 75–85, 92–103, 118–129, 135–143, 161–169.
[3]Analyzed using PROCHECK-NMR[42]

and ψ were created by using a ± 30° window on the predicted values of these angles[36]. Cα and Cβ chemical shifts were corrected for deuteration[37]. Distance restraints were obtained by converting integrated NOE peak intensities into distance upper limits using the macro CALIBA in DYANA v1.5 (ref. 38). The HN–HN and HN–Hα distance upper limits were calibrated individually by using d_{min} = 2.4 Å, d_{ave} = 3.6 Å and d_{max} = 5.5 Å and iteratively changing the scaling factor. Each hydrogen bond was represented by two distance upper limit restraints (N–O, HN–O) to preserve linear bond geometry. A total of 160 random structures were calculated[38] and subjected to one cycle of 4,000 steps of heating and 16,000 steps of annealing followed by 1,000 steps of conjugate gradient minimization. The 20 structures with the lowest target functions were selected. The resulting structures were subjected to 6,000 steps of conjugate gradient energy minimization *in vacuo*[39]. The 10 lowest energy structures were selected to represent the 3D fold of OmpA(0–176) in DPC micelles.

Coordinates. The structure has been deposited in the Protein Data Bank (accession number 1G90).

Acknowledgments
This work was supported by a grant from the NIH. The experiments at 750 MHz were carried out at the National Magnetic Resonance Facility at Madison, which is supported by the NIH and NSF.

Correspondence should be addressed to L.K.T. *email: lkt2e@virginia.edu*

Received 27 November, 2000; accepted 14 February, 2001.

1. Bax, A. *Curr. Op. Struct. Biol.* **4**, 738–744 (1994).
2. Gardner, K. H. & Kay, L.E. *Annu. Rev. Biomol. Struct.* **27**, 357–406 (1998).
3. MacKenzie, K.R., Prestegard J.H. & Engelman, D.M. *Science* **276,** 131–3 (1997).
4. Rastogi, V.K. & Girvin, M.E. *Nature* **402**, 263–8 (1999).
5. Ketchem, R.R., Hu, W. & Cross, T.A. *Science* **261**, 1457–1460 (1993).
6. Opella, S.J. *et al. Nature Struct. Biol.* **6**, 374–379 (1999).
7. Pervushin, K., Riek, R., Wider, G. & Wüthrich, K. *Proc. Natl. Acad. Sci. USA* **94**, 12366–12371 (1997).
8. Kay, L.E. & Gardner, K.H. *Curr. Opin. Struct. Biol.* **7**, 722–731 (1997).
9. Goto, N.K. & Kay, L.E. *Curr. Opin. Struct. Biol.* **10**, 585–592 (2000).
10. Tjandra, N. & Bax, A. *Science* **278**, 1111–1114 (1997).
11. Battiste, J.L. & Wagner G. *Biochemistry* **39**, 5355–5365 (2000).
12. Grisshammer, R., Averbeck, P. & Sohal, A.K. *Biochem. Soc. Trans.* **27**, 899–903 (1999).
13. Curran, A.R., Templer, R.H. & Booth, P.L. *Biochemistry* **38**, 9328–9336 (1999).
14. Sanders, C.R. & Nagy, J.K. *Curr. Opin. Struct. Biol.* **10**, 438–442 (2000).
15. Kleinschmidt, J.H., den Blaauwen, T., Driessen, A.J.M. & Tamm, L.K. *Biochemistry* **38**, 5006–5016 (1999).
16. Kleinschmidt, J.H., Wiener, M. & Tamm, L.K. *Protein Sci.* **8**, 2065–2071 (1999).
17. Arora, A., Rinehart, D., Szabo, G. & Tamm, L.K. *J. Biol. Chem.* **275**, 1594–1600 (2000).
18. Saint, N., El Hamel, C., De, E. & Molle, G. *FEMS Microbiol. Lett.* **190**, 261–265 (2000).
19. Belaaouaj, A., Kim, K.S. & Shapiro, S.D. *Science* **289**, 1185–1188 (2000).
20. Soulas, C. *et al. J. Immunol.* 165, 2335–2340 (2000).
21. Pautsch, A. & Schulz, G.E. *Nature Struct. Biol.* **5**, 1013–1017 (1998).
22. Pautsch, A. & Schulz, G.E. *J. Mol. Biol.* **298**, 273–282 (2000).
23. Schweizer, M., Hindennach, I., Garten,W. & Henning, U. *Eur. J. Biochem.* **82**, 211–217 (1978).
24. Dornmair, K., Kiefer, H. & Jähnig, F. *J. Biol. Chem.* **265**, 18907–18911 (1990).
25. Yang, D. & Kay, L.E. *J. Biomol. NMR* **13**, 3–9 (1999).
26. Yang, D. & Kay, L.E. *J. Am. Chem. Soc.* **121**, 2571–2575 (1999).
27. Powers, R. *et al. J. Mol. Biol.* **221**, 1081–1090 (1991).
28. Zhu, G., Kong, X. M., Sze, K.H. *J. Biomol. NMR* **13**, 77–81(1999).
29. Ikura, M., Bax, A., Clore, G.M. & Gronenborn, A.M. *J. Am. Chem. Soc.* **112**, 9020–9022 (1990).
30. Liu, W.M. *J. Mol. Biol.* **275**, 541–545 (1998).
31. Caffrey, M. *et al. J. Magn. Reson.* **135**, 368–372 (1998).
32. Vogel, H., Nilsson, L., Rigler, R., Voges, K.P. & Jung G. *Proc. Natl. Acad. Sci. USA* **85**, 5067–5071 (1988).
33. Brown, M.F., Seelig, J. & Häberlen, U. *J. Chem. Phys.* **70**, 5045–5053 (1979).
34. Waugh, D. *J. Biomol. NMR* **8**, 184–192 (1996).
35. Muchmore, D.C., McIntosh, L.P., Russell, C.B., Anderson, D.E. & Dahlquist, F.W. *Methods Enzymol.* **177**, 44–73 (1989).
36. Cornilescu, G., Delaglio, F. & Bax, A. *J. Biomol. NMR*, **13**, 289–302 (1999).
37. Gardner K.H., Rosen, M.K. & Kay L.E. *Biochemistry* **36**, 1389–1401 (1997).
38. Güntert, P., Mumenthaler, C. & Wüthrich, K. *J. Mol. Biol.* **273**, 283–298 (1997).
39. Luginbühl, P., Güntert, P., Billeter, M. & Wüthrich, K. *J. Biomol. NMR* **8**, 136–146 (1996).
40. Koradi, R., Billeter, M. & Wüthrich, K. *J. Mol. Graphics* **14**, 51–55 (1996).
41. Farrow, N.A. *et al. Biochemistry* **33**, 5984–6003 (2000).
42. Laskowski, R.A., Rullmann, J.A.C., MacArthur, M.W., Kaptein, R. & Thornton, J.M. *J. Biomol. NMR* **8**, 477–486 (1996).